0273-2289/97/63-65—0363$10.75

Effect of Impeller Geometry on Gas-Liquid Mass Transfer Coefficients in Filamentous Suspensions

SUNDEEP N. DRONAWAT, C. KURT SVIHLA, AND THOMAS R. HANLEY*

Department of Chemical Engineering, Speed Scientific School, University of Louisville, Louisville, KY 40292

ABSTRACT

Volumetric gas-liquid mass transfer coefficients were measured in suspensions of cellulose fibers with concentrations ranging from 0 to 20 g/L. The mass transfer coefficients were measured using the dynamic method. Results are presented for three different combinations of impellers at a variety of gassing rates and agitation speeds. Rheological properties of the cellulose fibers were also measured using the impeller viscometer method. Tests were conducted in a 20 L stirred-tank fermentor and in 65 L tank with a height to diameter ratio of 3:1. Power consumption was measured in both vessels. At low agitation rates, two Rushton turbines gave 20% better performance than the Rushton and hydrofoil combination and 40% better performance than the Rushton and propeller combination for oxygen transfer. At higher agitation rates, the Rushton and hydrofoil combination gave 14 and 25% better performance for oxygen transfer than two Rushton turbines and the Rushton and hydrofoil combination, respectively.

Index Entries: Filamentous suspensions; Gas-liquid mass transfer; non-Newtonian rheology.

INTRODUCTION

Submerged, aerobic industrial fermentations are usually carried out in sparged, agitated gas-liquid reactors. Mycelial fermentations, an important class of biochemical processes, present unique mixing prob-

*Author to whom all correspondence and reprint requests should be addressed.

lems due to non-Newtonian behavior, changes in the rate-controlling step, and relatively high oxygen demand *(1)*. High dissolved gas demand and the shear insensitivity of the mycelial cultures make agitated tanks a popular reactor choice. A lack of understanding of gas-liquid mass transfer has hindered optimization for these processes *(2)*. Few studies have been conducted to study the effect of impeller geometry on gas-liquid mass transfer in filamentous systems *(3)*. Previous studies conducted by these authors focused on the effects of mixing on gluconic acid production by *Aspergillus niger* in submerged culture *(4,5)*. In the present work, cellulose fibers were used to simulate the filamentous nature of *Aspergillus niger*. The aim of this study was to obtain experimental data for gas-liquid mass transfer coefficients in filamentous systems for three types of commonly used impellers.

Some previous studies have suggested that cellulose fiber suspensions exhibit rheological behavior similar to filamentous mycelial broths, although higher mass loadings are generally required *(3,5)*. This work presents the results of mass transfer coefficient measurements in a mechanically agitated fermentor of 20 L capacity for a range of fiber concentrations, agitation speeds, and gassing rates using three types of impellers (a six-bladed Rushton turbine, a hydrofoil, and a marine propeller). Experiments were also conducted in a 65 L tank equipped with three Rushton turbine impellers to study the effect of scale-up. The rheological behavior of the fiber suspensions was characterized using the impeller method *(5)*.

EXPERIMENTAL METHODS

The 20 L fermentor used in the tests was equipped with two agitators of diameter 0.069 m, four baffles, and a heating and cooling element. A liquid volume of 15 L was used in the fermentor. The 65 L Plexiglas vessel had a height to diameter ratio of 3:1 and a working volume of 63.7 liters. It was equipped with four baffles and three Rushton turbine impellers. Schematic diagrams of the two systems are shown in Fig. 1. Table 1 lists the dimensions of the impellers and tanks used.

The cellulose fibers used in the studies (Solka Floc, grade KS-1016 Fiber Sales and Development, Urbana, OH) had an average fiber length of 216 μm and were suspended in tap water. Fiber concentrations of 5, 10, 15, and 20 g/L were used at aeration rates of 5, 10, and 20 standard L per minute. Dissolved oxygen concentrations were measured with a polarographic electrode. Gas flow rates were measured using a mass flow meter and a rotameter. The dissolved oxygen probe was connected to a PC for data acquisition via a computer interface board.

A separate experimental apparatus was constructed to measure the dynamics of the electrode. The schematic of the experiment is given in Fig. 2. In this experiment the polarographic electrode was placed in the tube and an arrangement for instantaneous change from nitrogenated

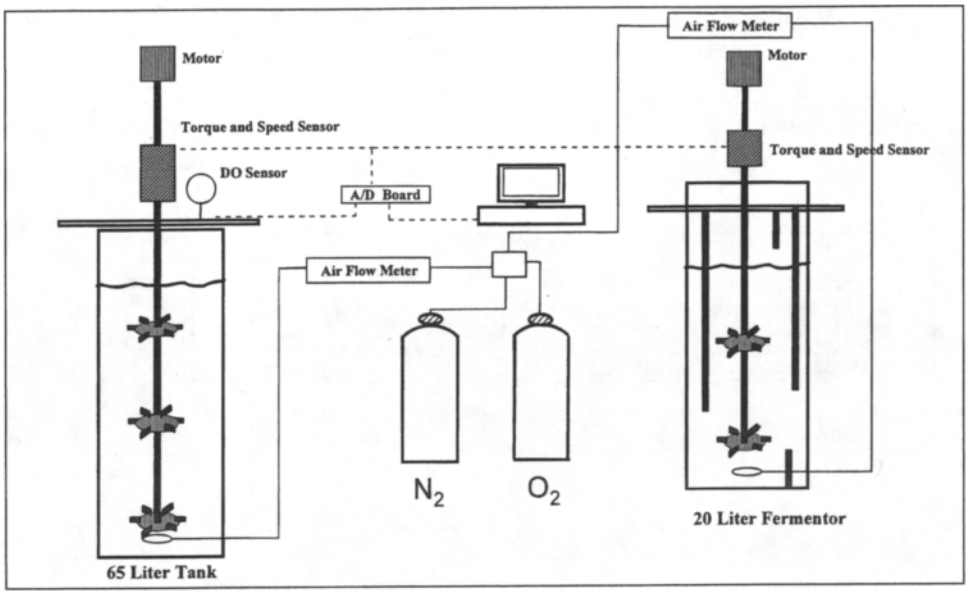

Fig. 1. Experimental setup for k_La and power measurements in the 20 L fermentor and 65 L tank.

Table 1
Dimensions of the Tanks and Impellers Used

20 Liter Fermentor		65 Liter Tank	
Diameter of Tank	22.5 cm	Diameter of Tank	30 cm
Height of Tank	50 cm	Height of Tank	106.7 cm
No of Baffles	4	No of Baffles	4
No. of Impellers	2	No. of Impellers	3
Baffle Width	2.0 cm	Baffle Width	2.85 cm
Impeller Diameter	6.9 cm	Impeller Diameter	9.9 cm

liquid to oxygenated liquid was constructed. The probe response was assumed to be linear and to be described by a second-order differential equation. A 386-microprocessor, 25 MHz computer was used for all trials and data analysis.

Volumetric gas-liquid mass transfer coefficients were measured using the polarographic electrode for which the dynamics were determined using the apparatus shown in Fig. 2. The dynamic method was used with an instantaneous interchange in inlet gas *(6)*. The tank was initially sparged with nitrogen gas for sufficient amount of time to attain saturation. Oxygen was then sparged to the tank and the dissolved oxygen

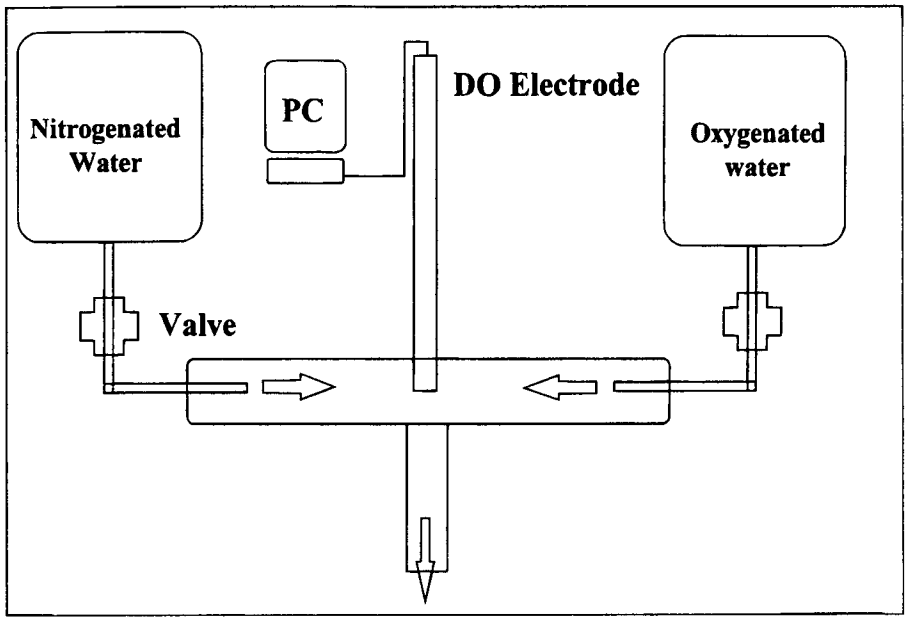

Fig. 2. Experimental setup for electrode dynamics.

concentration response measured at intervals of 0.10 s through the A/D interface. The measured dissolved oxygen concentration response curve was used to determine the value of k_La for the tests using the mathematical model discussed later in the paper. The temperature for all trials was maintained constant at 30°C.

The rheological behavior of the fiber suspensions were characterized using the impeller viscometer method for fiber concentrations varying from 10 to 30 g/L. The method for measurement of rheological properties of filamentous suspensions is described elsewhere *(4,5,7)*.

MATHEMATICAL MODEL

In the model derivation, the liquid phase is assumed to be well-mixed and the gas interchange from nitrogen to oxygen is assumed to take place instantaneously. The initial period in which both oxygen and nitrogen are present in the fermentor is not considered. Henry's law is assumed to apply at the gas-liquid interface *(3)*. The material balance for the liquid phase is:

$$\frac{dC_L}{dt} = k_La(\alpha C_g - C_L) \quad (1)$$

where α is the Henry's law coefficient.

The electrode dynamics are assumed to be described by a second-order differential equation with time constants τ_1 and τ_2. When expressed in the dimensionless form:

$$\phi = \frac{C_E(T) - C_E}{C_E(T) - C_E(0)} \quad (2)$$

the probe response in the electrode dynamic tests depends only on the dynamic characteristics, τ_1 and τ_2.

A solution for the measured dissolved oxygen response to a step change in inlet gas concentration can be obtained using Laplace transforms:

$$\frac{C_E s}{C_E(T) - C_E(0)} = \frac{e^{-\tau} ds}{\left(\frac{s}{k_L a} + 1\right)(\tau_1 s + 1)(\tau_2 s + 1)} \quad (3)$$

where a time lag τ_d has also been introduced. When this expression is inverted into the time domain, the resulting expression is a function only of the dynamic characteristics of the system.

The two time constants, τ_1 and τ_2, were determined by a nonlinear least squares regression of the electrode response curve. Since the probe dynamics did vary over time, the dynamics were determined just before or after a given set of trials. The dead time was obtained for each test by observing the plot of time vs the electrode response and the first observable electrode response was noted. The time axis was shifted by the value of the dead time determined for each trial. Since the electrode time constants τ_1 and τ_2 were determined in separate tests and τ_d found from direct inspection of the response curve; $k_L a$ is the only variable that is adjusted to fit the dynamic test data to the model.

RESULTS

The electrode time constants, τ_1 and τ_2, were typically in the range of 5.1 to 5.9 s, and 7.9 to 8.6 s, respectively. The largest $k_L a$ value for any absorption test was approx 0.036 s^{-1}, hence the electrode dynamics never dominated the overall response. The fit of the experimental data to the model was generally good as is shown in Fig. 3. The effect of cellulose fiber concentration on $k_L a$ for the Rushton and Rushton turbine combination for 10 L per minute air flow rate in the 20 L fermentor is presented in Fig. 4. It can be inferred from Fig. 4 that an increase in cellulose fiber concentration decreases the $k_L a$. This effect is more pronounced at higher agitation rates and higher concentrations of cellulose fiber. The effect of impeller geometry on the gas-liquid mass transfer coefficient is shown in Figs. 5 and 6 for cellulose fiber concentrations of 10 g/L and 20 g/L, respectively for 10 L per minute air-flow rate. The increase in cellulose fiber concentration decreases the gas-liquid mass transfer coefficient for all combinations of impellers. Similar behavior was observed at an air flow rate of 20 L per minute. It is evident that the gas-liquid mass transfer coefficient increases with an increase in aeration rate. Figures 7 and 8 show the effect of impeller geometry on power consumption at 10 L per minute and 20 L per minute

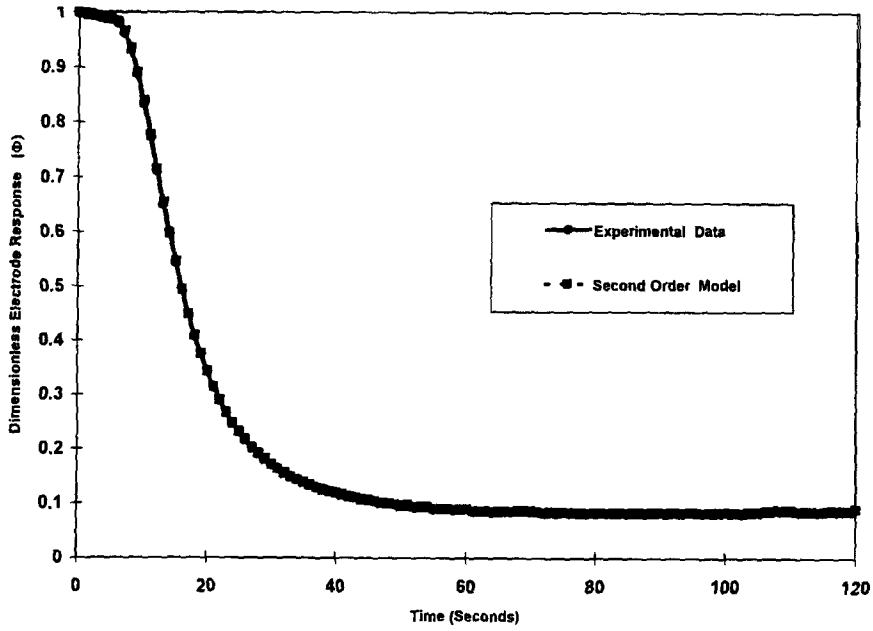

Fig. 3. Experimental electrode response fit to the model for k_La measurements.

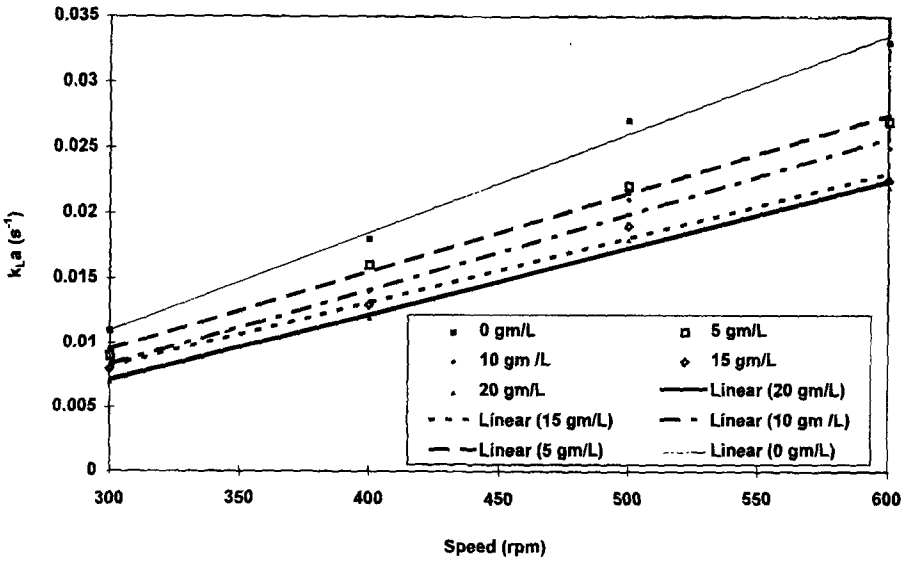

Fig. 4. Effect of fiber conc. on k_La at 10 lpm airflow rate for Rushton and Rushton (20 L fermentor).

flow rate, respectively with no cellulose fibers. Figures 9 and 10 show the effect of solids concentration on the gas-liquid mass transfer coefficient at air flow rates of 10 L per minute and 20 L per minute, respectively in the 65 L tank. Figure 11 shows the rheological properties of the cellulose fiber suspension measured using the impeller method. Table 2 lists the power law parameters for the cellulose fiber suspensions.

Table 2
Power Law Parameters for Cellulosic Fiber Suspensions

Fiber Concentration	n	kpl
10	0.458	1.24
20	0.401	1.82
30	0.283	3.09

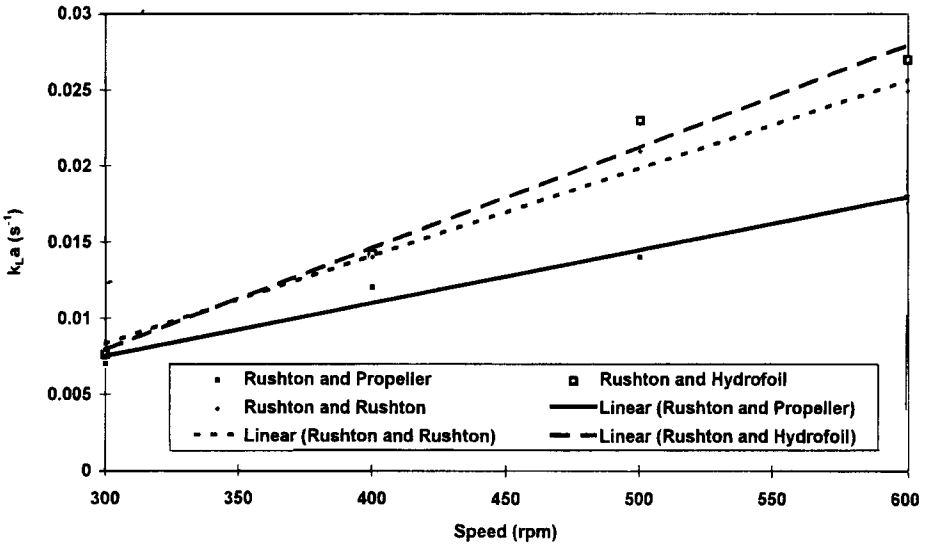

Fig. 5. Effect of impeller geometry on k_La at 10 lpm airflow rate and fiber conc. of 10 g/L (20 L fermentor).

DISCUSSION

The technique used to measure the gas-liquid mass transfer coefficient was consistent. The gas-liquid mass transfer coefficients decreased as the fiber concentrations increased, as expected.

At low agitation rates and with no fibers present, all three combinations of impellers performed similarly in the 20 L fermentor. The k_La values increased with increasing agitation for all three combinations of impellers. At higher fiber concentrations, the combination of a Rushton turbine and hydrofoil was more effective and had a higher k_La value than other combinations. At lower agitation rates the two Rushton turbines gave better performance for the conditions studied. The effect of solids concentration on k_La was also studied in the 65 L tank at 10 L per minute and 20 L per minute. From the results, it is evident that the k_La decreases with an increase in solids concentration.

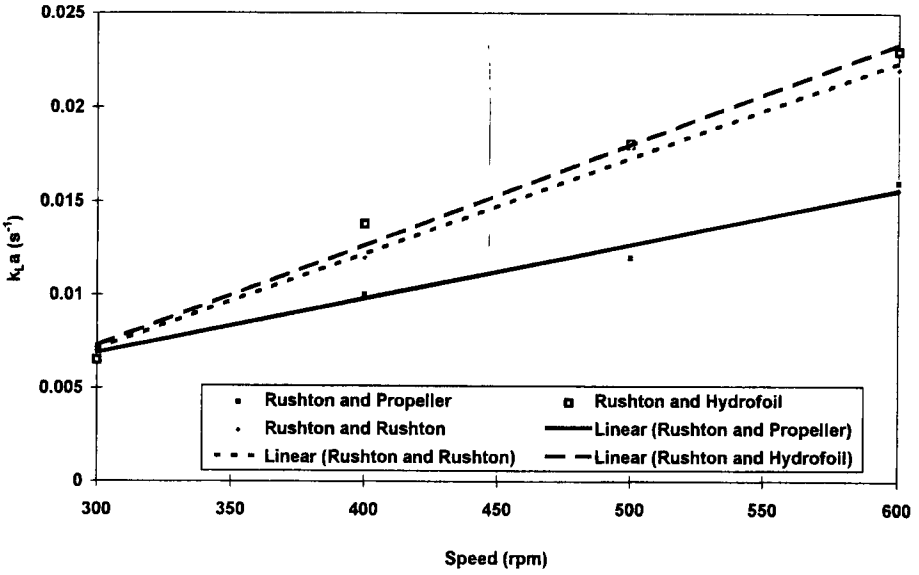

Fig. 6. Effect of impeller geometry on k_La at 10 lpm airflow rate and fiber conc. of 20 g/L (20L fermentor).

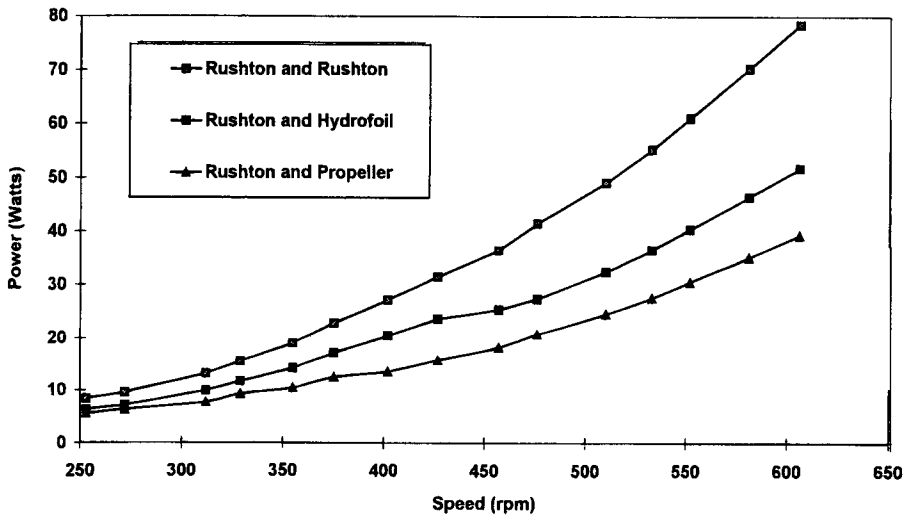

Fig. 7. Effect of impeller geometry on power at 10 lpm airflow rate (20 L fermentor).

The reduction in oxygen transfer that occurs in fermentations involving filamentous mycelial broths is postulated to be the result of viscous, shear-thinning broth rheology. The fibers used in these tests are straight and unbranched and hence are imperfect models of mycelial hypae. Although the measured viscosity of the suspensions increased with increasing fiber concentration, the effect was not nearly as large as that reported for filamentous mycelial broths at similar mass loadings. The presence of solids in the liquid phase can cause a decrease in the mass

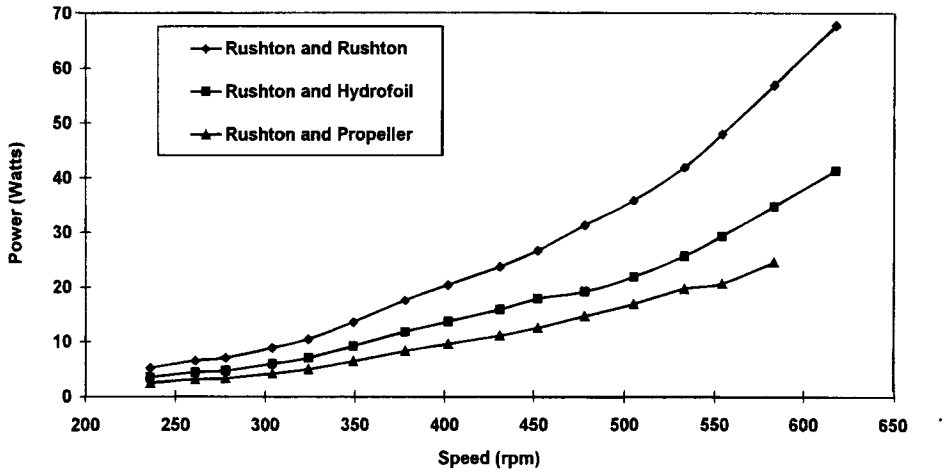

Fig. 8. Effect of impeller geometry on power at 20 lpm airflow rate (20 L fermentor).

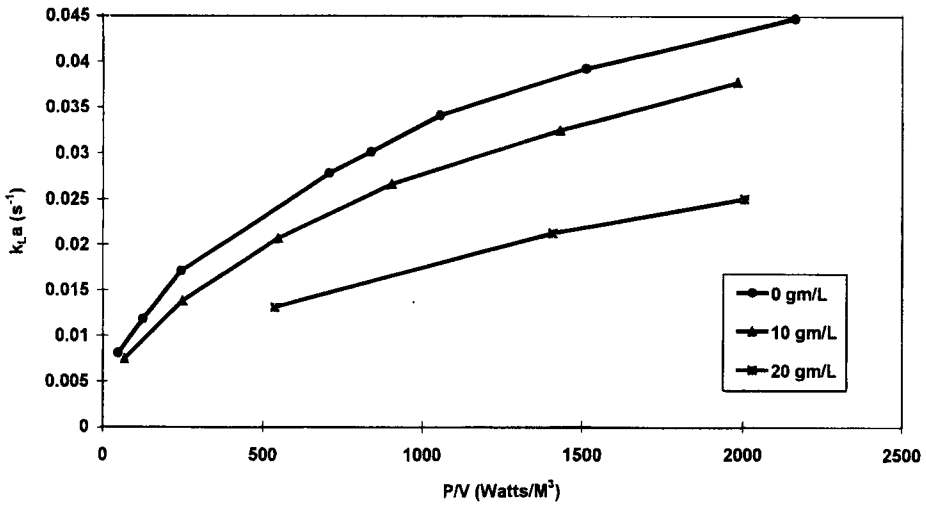

Fig. 9. Effect of solids concentration on k_La at 10 lpm airflow rate (65 L tank).

transfer coefficient even if the viscosity is similar to that of water, perhaps by acting as sites for bubble coalescence, thus decreasing the interfacial area *(3)*, or by damping the level of turbulence in the liquid.

From the results of the power measurements, it is evident that the combination of two Rushton turbines consumes the most power in the 20 L fermentor. This effect is more evident at higher agitation rates. Similar effects were observed by many workers *(7,8)* who reported the power draw to double when impeller speed was doubled. The power draw increases since the energy is spent on liquid circulation and not for gas dispersion. Once the gas has been dispersed and is well-mixed in the fermentor, increasing the agitation will result in only a slight increase in the mixed fraction of the gas. At lower agitation rates, the gas tends to accumulate

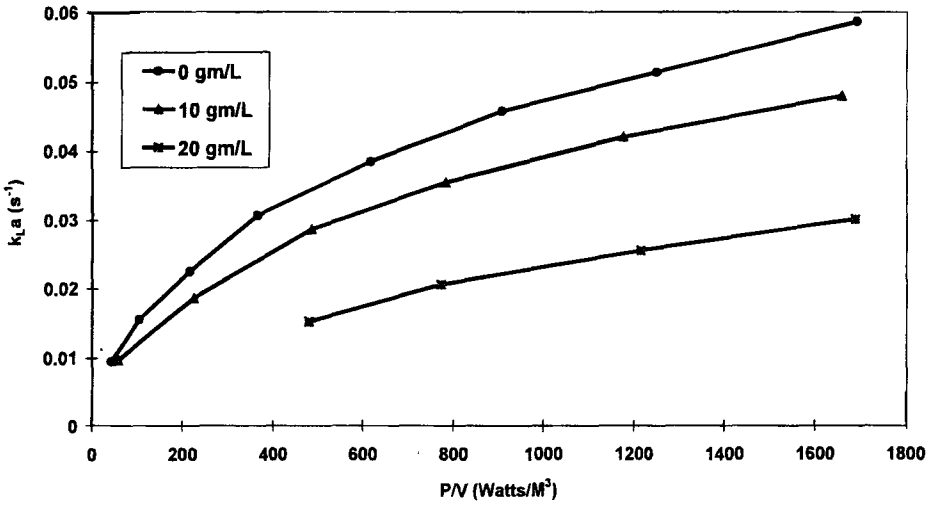

Fig. 10. Effect of cellulose fibers on k_La at 20 lpm airflow rate (65 L tank).

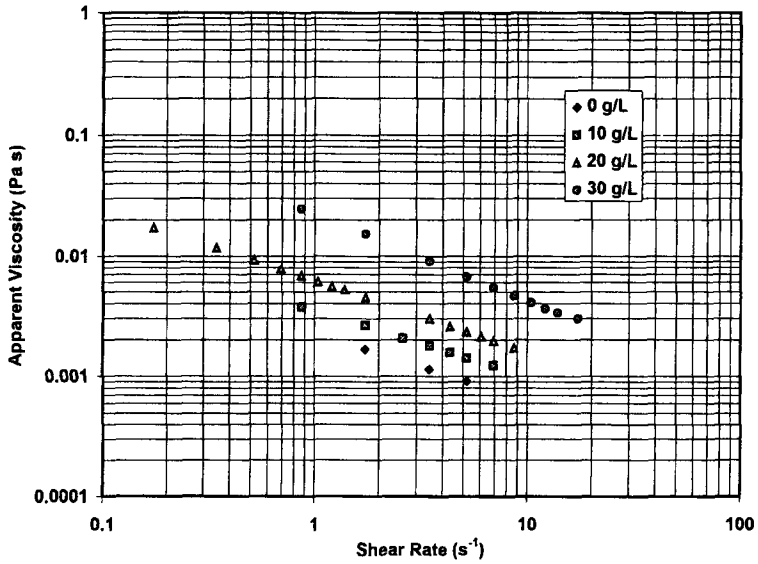

Fig. 11. Apparent viscosity data for cellulosic fiber suspensions.

near impellers with less circulation, which results in a decrease in the mixed fraction of gas. By increasing the gas flow rate from 10 to 20 L per minute, there was a slight decrease in power consumption, but the trends were similar to the results at 10 L per minute.

CONCLUSIONS

The conclusions made are limited to the two tank sizes, the three impellers, the fiber type and concentrations, and the aeration and agitation rates used in this investigation. In the 20 L fermentor at low agitation rates

the two Rushton turbines gave 20% better performance than the Rushton and hydrofoil combination and 40% better performance than the Rushton and propeller combination. At higher agitation rates, the Rushton and hydrofoil combination gave 14% better performance than two Rushton turbines, and 25% better performance than the Rushton and hydrofoil combination. The power consumption with the Rushton and propeller combination was 57% less than the power consumption with two Rushton turbines. The power consumption with the Rushton and hydrofoil combination was 35% less than that of the two Rushton turbine combination.

NOTATION

k_La	gas liquid mass transfer coefficient (s^{-1})
C_g	gas side concentration
C_L	liquid side concentration
$C_E(0)$	electrode response at time = 0
$C_E(T)$	electrode response at time = t
ϕ	dimensionless electrode response
α	Henrys law coefficient
τ_1	time constant
τ_2	time constant
τ_d	dead time

REFERENCES

1. Moo-Young, M. and Blanch, H. W. (1981), *Adv. Biochem. Eng.* **19,** 1–69.
2. Chisti, M. Y. and Moo-Young, M. (1988), *Biotechnol. Bioeng.* **31,** 487.
3. Svihla, C. K. and Hanley, T. R. (1992), *AIChE Symposium Series,* **88,** 114–118.
4. Dronawat, S. N., Svihla, C. K., and Hanley, T. R. (1995), *Appl. Biochem. Biotechnol.* **51/52,** 347–354.
5. Svihla C. K., Dronawat, S. N., and Hanley, T. R. (1995), *Appl. Biochem. Biotechnol.* **51/52,** 355–366.
6. Linek, V., Vacek, V., and Benes, P. (1988), *Chem Eng. J.* **34,** 11.
7. Dronawat, S. N, (1996), Mixing in Fermentors: Analysis of Oxygen Transfer and Rheology, *Ph. D. Dissertation,* University of Louisville.
8. Laine, J. and Kuoppamaki, R. (1979), *Ind. Chem. Process Des. Dev.,* **18,** 501–550.